Mode I and Mode II Interlaminar Fracture Behavior of Glass Woven Fabric Composites

M.Kotaki[1], T.Kuriyama[1], H.Hamada[2], Z.Maekawa[2] and I.Narisawa[1]

[1]*Department of Material Science and Engineering, College of Engineering, Yamagata University, Jonan, Yonezawa 992-8510, Japan*

[2]*Advanced Fibro Science, Kyoto Institute of Technology, Matsugasaki, Sakyo-ku, Kyoto 606-8585, Japan*

ABSTRACT

Mode I and mode II interlaminar fracture behavior was investigated on laminated composites reinforced with plain glass woven fabrics that were treated with different concentrations of silane. In the mode I fracture, the low silane concentration specimen showed higher fracture toughness than the high silane concentration specimen. This is due to the occurrence of the micro crack in the fiber strands. In the low silane concentration specimen, larger damage zone due to the micro crack was formed ahead of the crack tip. In the mode II fracture, on the contrary, the fracture toughness increased with increasing silane concentration, and no significant damage zone for the fracture toughness was formed ahead of the crack tip.

1. INTRODUCTION

Woven fabric composites have been widely used in composite fields, especially as printed circuit boards in the electronics industry. The most important performance required in the printed circuit boards is heat resistance, as well as dimensional stability and resin impregnation, because interlaminar delamination and debonding between glass fiber fabrics and matrix resin often occur by the thermal effect during the printed wiring manufacturing process. For other applications of the woven fabric composites, the delamination occurs due to mechanical stress. In practical applications, the delamination between plies is a fatal problem, as it is for the other laminated type composites.

A numbers of works have been conducted on the delamination behavior of the laminated composites, especially for unidirectional laminates, since the 1980s. To improve the delamination resistance, several thermoplastic resins /1,2,3,4,5/ and rubber-modified epoxies /6,7,8,9/ have been used as matrix resin, and also other techniques such as interleaving /10,11/ and stitching /12,13/ have also been successful. The mechanisms of the interlaminar fracture behavior of the unidirectional laminated composites have been identified using several microscopy observation techniques. The factors for the interlaminar fracture resistance were, for example, the size of the deformation zone ahead of the crack tip/14/, the formation of fiber bridging behind the propagating crack tip/5,15/ and the adhesive strength of the fiber/matrix interface/14/. Several investigations also have been conducted on the delamination behavior of the woven fabric composites with higher delamination resistance compared to the unidirectional composites /16,17,18,19,20,21,22,23,24/. The papers were mainly concerned with the effects of weaving pattern and delamination direction, and very few papers have dealt with interfacial adhesion between fiber and matrix. The mechanisms of the interlaminar fracture of the woven fabric composites have not been well identified compared to the unidirectional composites, because of their complex architectures of the woven fabrics and the lack of detailed observation of the crack tip.

Silane coupling agents are used as finishing agents for glass fiber in the composite fields in order to obtain good interfacial adhesion between the reinforcement and matrix resin, because the interfacial adhesion greatly affects the mechanical properties of the composite materials. Due to the rapidly expanding application of composite materials in many engineering constructions, the issue of interface is a major concern in design and manufacture of composite materials. Several common experimental techniques have been developed to assess the fiber / matrix interfacial bond quality, in the so-called "single fiber composite tests" /25,26,27,28,29,30,31,32,33/. However, it is difficult to apply the experimental data obtained from these model composite tests to the composite materials used in practical applications. Therefore, the interfacial effects on the mechanical performance of the actual composite materials must be well investigated for practical engineering fields.

In this study, the mode I and mode II interlaminar fracture behavior have been investigated in glass woven fabric composites. The mechanisms of the mode I and mode II interlaminar fracture of the woven fabric composites that included the effects of silane concentration treated on glass fiber fabrics have been discussed by means of the detailed observation of the part ahead of the crack tip during the fracture toughness tests using an optical microscope.

2. EXPERIMENTAL

2-1 Materials

Materials used in this paper were plain glass woven fabrics of 44 (warp) x 34 (weft) strands count over inch (WE18W: Nitto Boseki Co., Ltd., Japan) as reinforcement. The fiber strands from the E-glass fiber fabric consisted of 400 glass fiber filaments with 9 μm diameter. Surface treatment was performed on the glass fiber fabrics using γ-methacryloxypropyltrimethoxy-silane (A-174: Nippon Unicar Company, Japan) referred to as MPS. The aqueous solutions of the MPS were acidified with acetic acid at pH = 4.0. The glass fiber fabrics were dipped into the MPS aqueous solutions. They were squeezed between squeeze rollers and dried at 110 °C for 10 min. The concentration of the MPS was 0.01, 0.4 and 1.0wt%.

The matrix resin used was a bisphenol A type vinyl ester resin (R-806; Showa Highpolymer Co., Ltd., Japan), which included styrene monomer of approximately 45wt%. The room temperature catalyst used was 0.7 phr methylethylketoneperoxide (MEKPO) promoted by 0.3 phr cobalt naphthenate solution. Twenty-ply composite laminates of 4mm thickness were fabricated by hand lay-up technique. The composite laminates were cured at 80°C for 3h and at 150°C for 2h. then at room temperature for 48h. Fiber volume fraction in each laminate was approximately 40 %.

2-2 Fracture Toughness Tests

Mode I and mode II interlaminar fracture toughness tests were carried out using double cantilever beam (DCB) and end notched flexure (ENF) specimens as shown in Fig. 1. The DCB and ENF specimens were cut

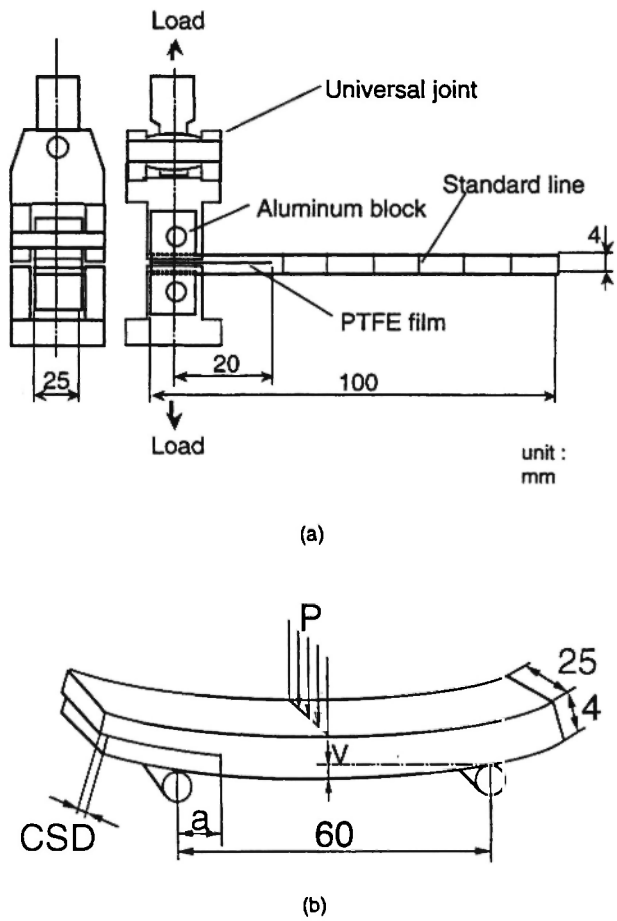

Fig. 1: Geometry of (a) DCB and (b) ENF specimens.

parallel to the weft fiber direction, with 100 mm length and 25 mm width. Initial defects of the DCB and ENF specimens were introduced by inserting PTFE film with 40 μm thickness during molding the laminates.

The fracture toughness tests were carried out under a stroke rate of 1.0 mm/min for mode I and 0.1 mm/min for mode II using a Shimadzu Autograph universal testing machine. The crack length was measured on one side of the specimen with traveling microscope at a magnification of x100 during the DCB tests. Displacement of the testing machine was used as the crack opening displacement (COD) on the load line for the DCB tests. Mode I and mode II interlaminar fracture toughness values were calculated at the load points for the visual initiation and propagation of cracks in accordance with JIS K7086/34/.

Acoustic emission (AE) activity was measured during the DCB tests. The gain and the threshold values were 60 dB and 0.33V, respectively. The crack propagation behavior was observed by means of an optical microscope (OM) and scanning electron microscope (SEM).

3. RESULTS

3-1 Mode I Fracture Behavior

Figure 2 shows load-displacement curves with AE counts in the mode I fracture toughness tests of plain glass woven fabric composites. The lower MPS concentration (0.01wt%) specimens indicated stable fracture behavior, whereas the higher MPS concentration (0.4wt% and 1.0wt%) specimens showed unstable fracture behavior. In the case of the stable fracture behavior, many AE counts were detected during the DCB tests. On the other hand, the number of AE counts in the unstable fracture behavior was much smaller compared to the stable fracture behavior, then the streaks of AE counts were detected at the onset of the unstable fracture in which the load suddenly decreased in the load-displacement curves. In the initial load-displacement curves, the AE counts started to be detected at approximately onset of non-linearity in the initial load-displacement curves regardless of the MPS concentration. AE measurement is a useful technique for the determination of the onset of non-linearity in the

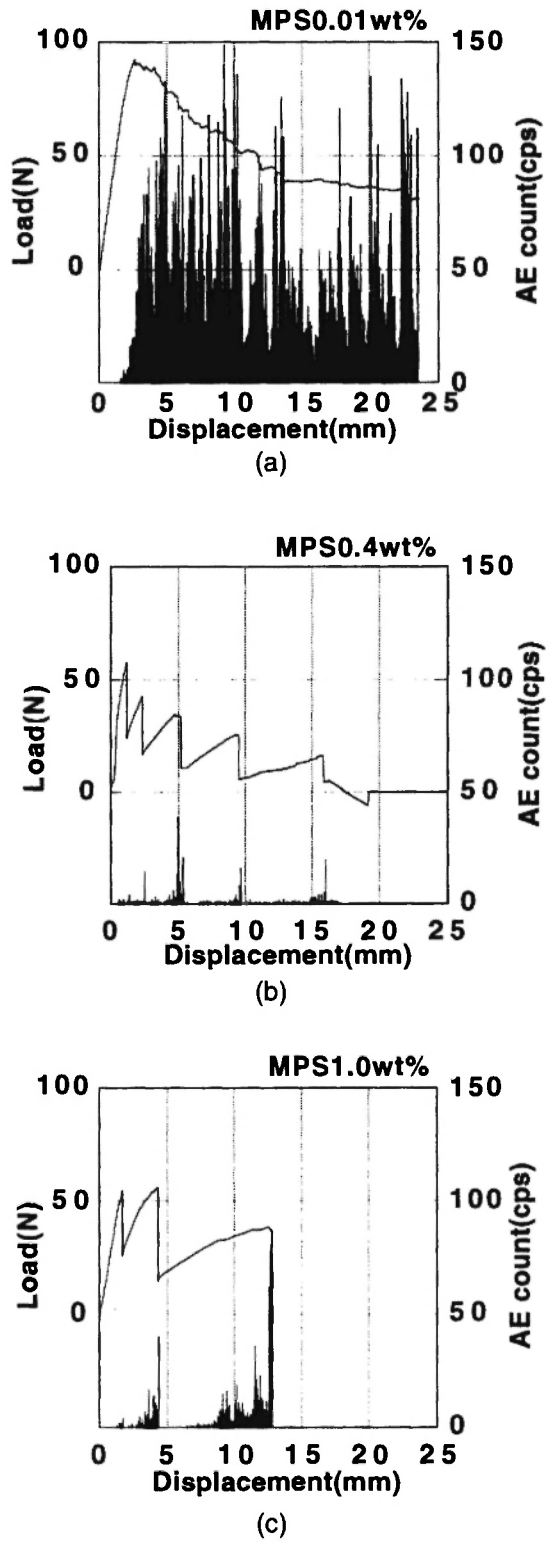

Fig. 2: Load-displacement curves with AE counts of mode I fracture toughness tests of plain glass woven fabric composites; (a) MPS 0.01wt%, (b) MPS 0.4wt% and (c) MPS 1.0wt%.

mode I interlaminar fracture toughness tests of woven fabric composites.

The relations between mode I fracture toughness and crack extension, R-curves, are shown in Fig. 3. The fracture toughness increased with increasing crack extension from the initial crack in every type of specimen. Then fracture toughness reached plateau values in the case of the lower MPS concentration specimens which indicated stable crack growth behavior. In the higher MPS concentration specimens, however, the R-curves displayed saw-teeth-like behavior due to the occurrence of the unstable fracture.

Figures 4 and 5 show OM micrographs for the part ahead of the initial crack tip for 0.01wt% and 1.0wt% specimens when the DCB tests were interrupted at the onset of non-linearity and maximum load points in the initial load-displacement curves. The OM micrographs were viewed in a bright field for thin sections. In the lower MPS concentration, the crack initiation occurred from the tip of an initial crack film to fiber strand at the onset of non-linearity. Then, many micro cracks occurred in the fiber strands and formed a large damage zone ahead of the crack tip from the onset of non-linearity to the maximum load point. In the higher MPS concentration, the crack also initiated to occur into the resin rich region between plies at the onset of non-linearity. The crack did not clearly show further crack propagation until the maximum load point, and then the crack propagated into the resin rich region at the maximum load point, i.e. the unstable fracture occurred.

SEM micrographs for the cross sections of the edge of DCB specimens in the crack propagation region are shown in Fig. 6. The crack propagating direction was from left to right hand side in all of the SEM micrographs. In the lower MPS concentration specimens many micro cracks and sub-cracks were observed in the fiber strands, but no micro crack occurred in the fiber strand and the crack ran into the resin region between plies in the higher MPS concentration specimens including MPS 0.4wt% specimen. Fig.7 shows SEM micrographs of the fiber surface on the mode I fracture surface. In the lower MPS concentration specimens, no resin was observed on the fiber surface. However, much resin adhered on the fiber surface in the higher MPS concentration specimens. This is attributed to the improvement of the

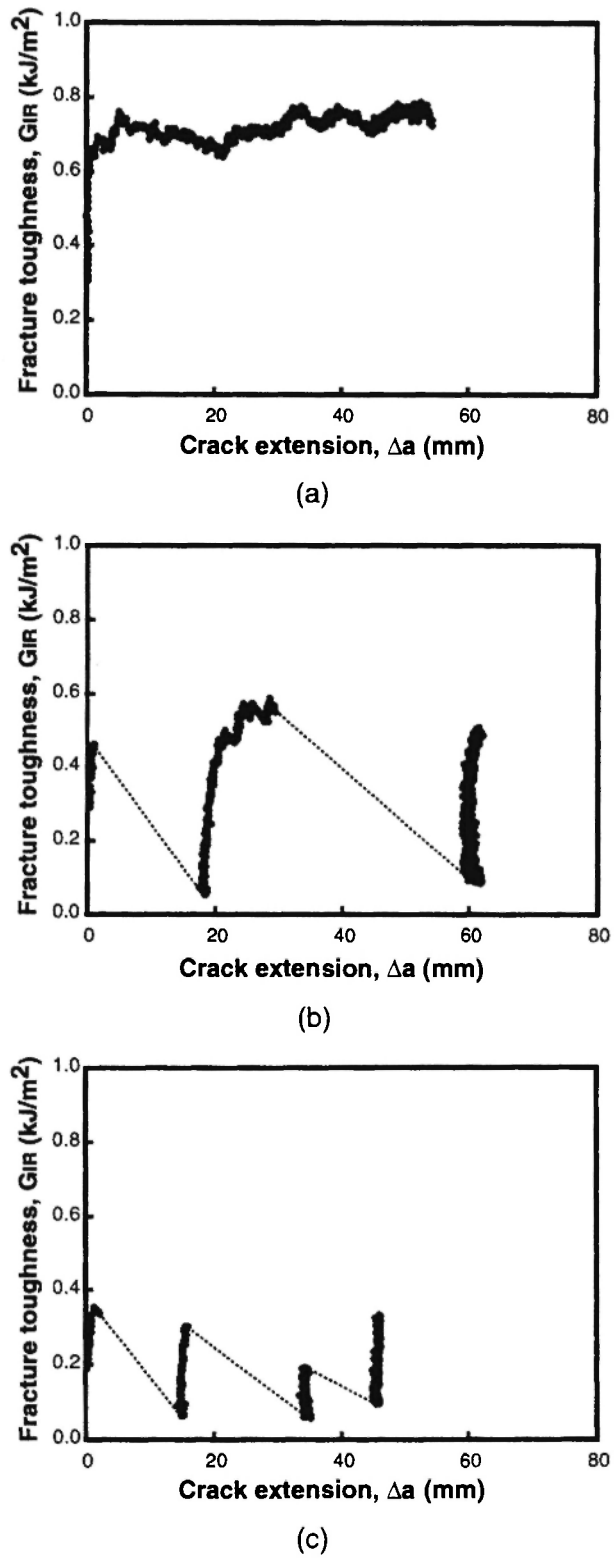

Fig. 3: R-curves of mode I fracture toughness tests of plain glass woven fabric composites; (a) MPS 0.01wt%, (b) MPS 0.4wt% and (c) MPS 1.0wt%.

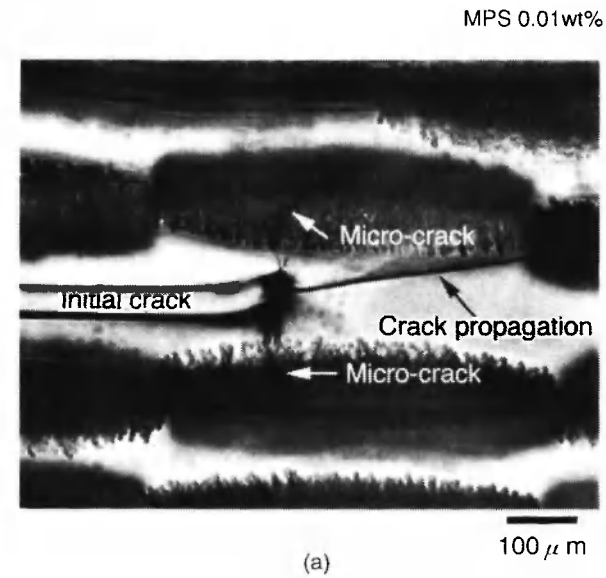

Fig. 4: OM micrographs of the damage zone ahead of initial crack tip in mode I crack initiation for MPS 0.01wt% specimen of plain glass woven fabric composites; at (a) the onset of non-linearity and (b) maximum load point.

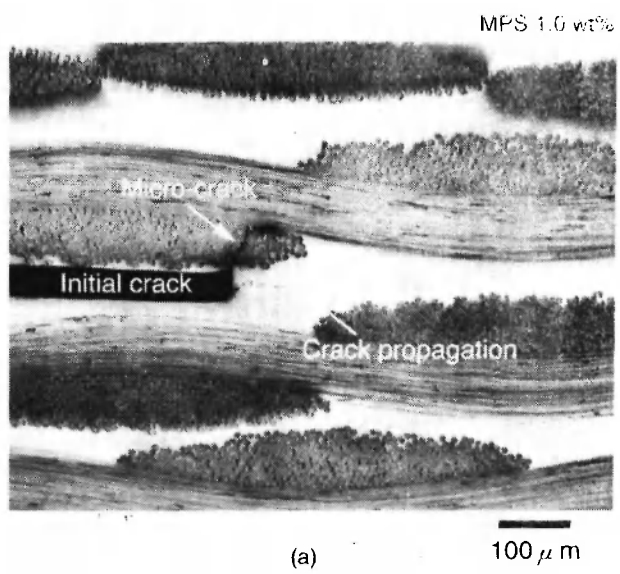

Fig. 5: OM micrographs of the damage zone ahead of initial crack tip in mode I crack initiation for MPS 1.0wt% specimen of plain glass woven fabric composites; at (a) the onset of non-linearity and (b) maximum load point.

interfacial adhesion between fiber and matrix by increasing the MPS concentration.

The initiation values of mode I fracture toughness, G_{IC}, calculated at the onset of non-linear and the maximum load point in the initial load-displacement curves as a function of the MPS concentration are shown in Fig. 8. From the OM observations, the G_{IC} values indicated the mode I fracture toughness corresponding to the initiation of the actual crack occurrence at the onset of non-linearity and the propagation of the main crack at the maximum load points, respectively. Both of the G_{IC} values decreased

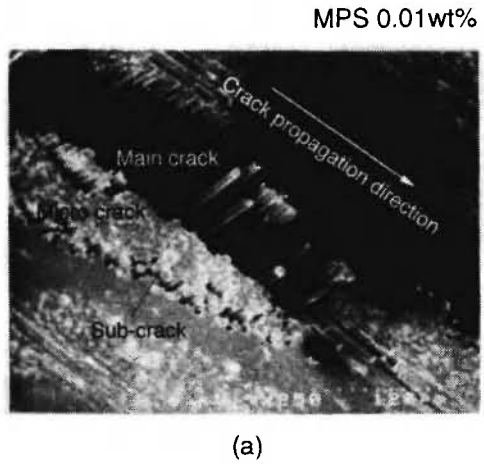

Fig. 6: SEM micrographs of the cross sections of DCB specimens after mode I interlaminar crack propagation of plain glass woven fabric composites; (a) MPS 0.01wt%, (b) MPS 0.4wt% and (c) MPS 1.0wt%.

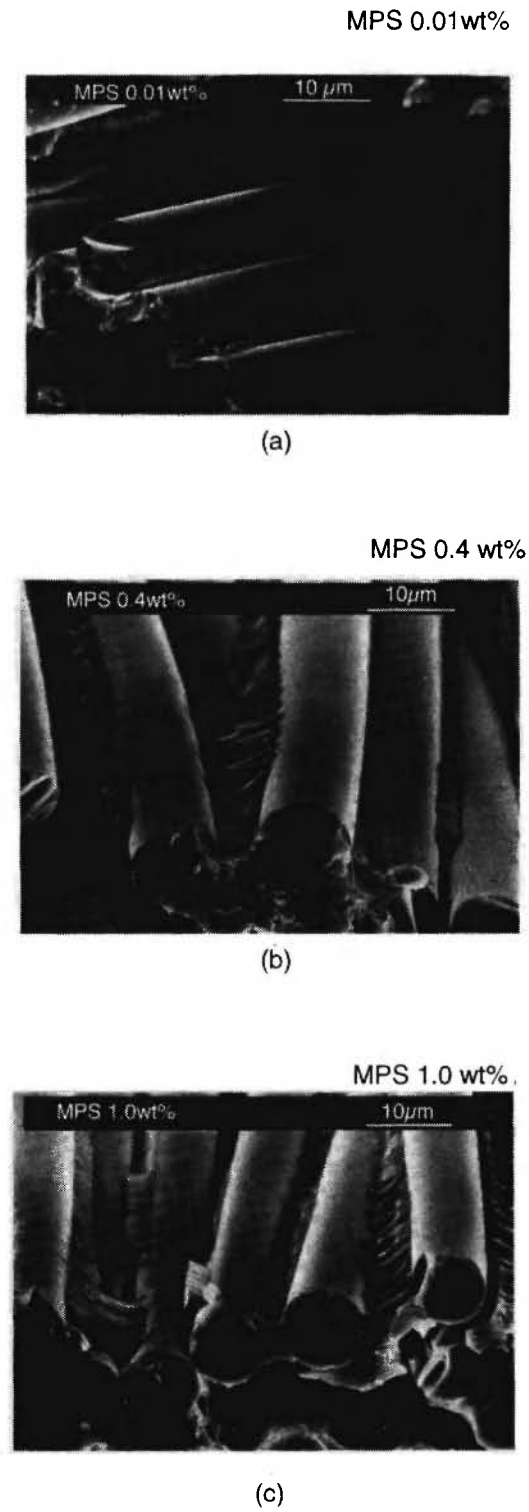

Fig. 7: SEM micrographs of fiber surface on mode I fracture surface of plain glass woven fabric composites; (a) MPS 0.01wt%, (b) MPS 0.4wt% and (c) MPS 1.0wt%.

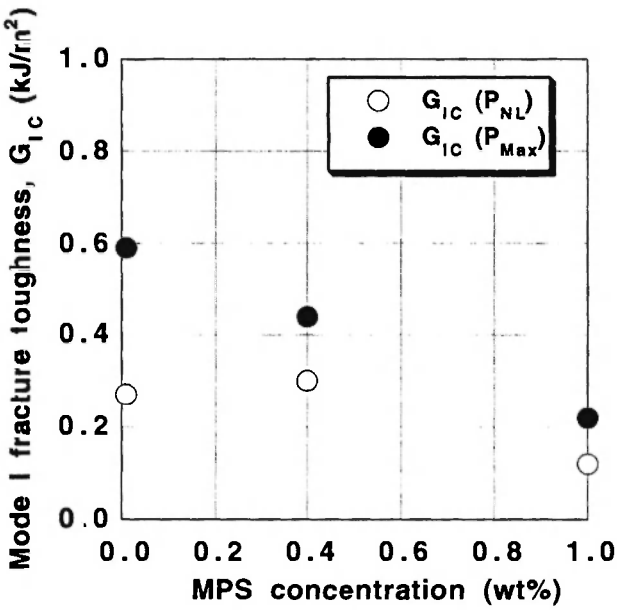

Fig. 8: Relation between initiation values of mode I fracture toughness and MPS concentration of plain glass woven fabric composites.

with increasing MPS concentration, but the tendency was more remarkable in the G_{IC} at the maximum load points.

The difference of the G_{IC} calculated at between the onset of non-linearity and the maximum load point in the initial load-displacement curves, ΔG_I, as a function of MPS concentration is shown in Fig. 9. In the OM

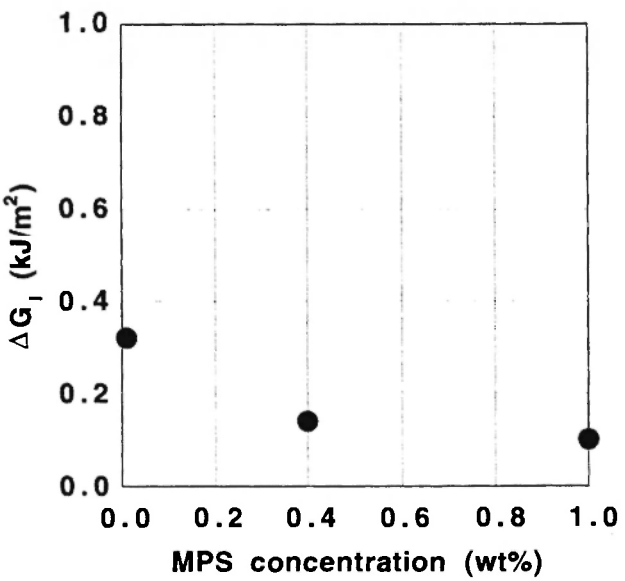

Fig. 9: Relation between ΔG_I and MPS concentration of plain glass woven fabric composites.

observations, the main crack that started to occur at the onset of non-linearity arrested until maximum load point. Therefore, the ΔG_I values represented the fracture energy spent for forming the damage zone ahead of the crack tip from the initiation of the crack occurrence to the propagation of the main crack. The ΔG_I decreased with increasing MPS concentration, i.e. the fracture energy for forming the damage zone ahead of the crack tip until the onset of the crack propagation decreased with increasing MPS concentration.

3-2 Mode II Fracture Behavior

Load-displacement curves of the mode II fracture toughness tests are shown in Fig. 10. The compliance of the initial load-displacement curve decreased when MPS concentration increased, and the load at the onset of non-linearity also increased when MPS concentration increased.

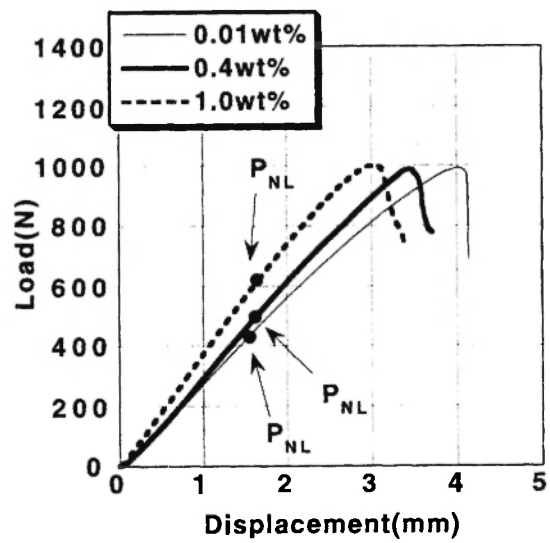

Fig. 10: Load – displacement curves of mode II fracture toughness tests for plain glass woven fabric composites.

The OM observation was conducted on the part ahead of the initial crack tip for the 1.0wt% specimen when the ENF tests were interrupted at each point between the initiation and the maximum load point including the onset of non-linearity in the initial load-displacement curves. The polished surface of the edge of the ENF specimens was observed using optical

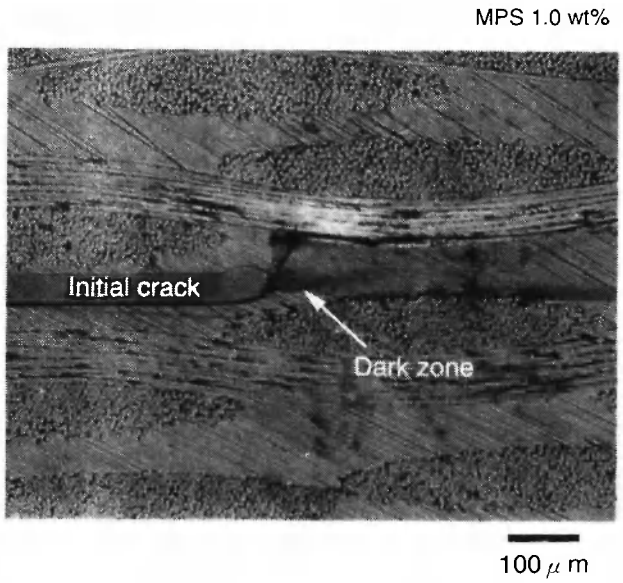

Fig. 11: OM micrograph of the part ahead of initial crack tip at the onset of the non-linearity in mode II crack initiation for MPS 1.0wt% specimen of plain glass woven fabric composites.

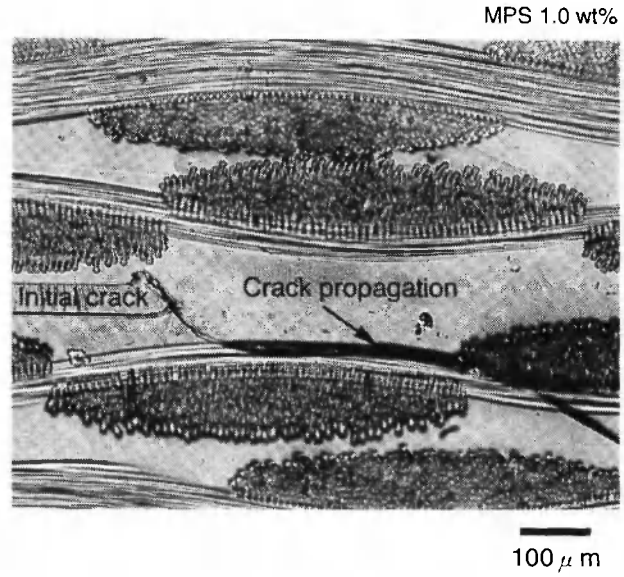

Fig. 12: OM micrograph of the part ahead of initial crack tip at the onset of the non-linearity in mode II crack initiation for MPS 1.0wt% specimen of plain glass woven fabric composites; viewed in bright field for a thin section.

microscope. Fig. 11 shows OM micrograph of the crack tip at the onset of non-linearity.

The dark zone ahead of the initial crack tip was observed at the onset of non-linearity, and then the crack slowly propagated across the fiber strand until the maximum load point. The crack propagation speed rapidly increased at the maximum load point. A thin section sample for the dark zone after the onset of non-linearity was prepared for the OM observation, in order to identify the substance of the dark zone. The bright field image of the OM observation for the thin section sample is shown in Fig. 12. The crack propagation across the fiber strand was clearly observed; however, the dark zone was not detected. OM observation in a cross-polarized light was also conducted, but no shear deformation zone was observed ahead of the crack tip. Therefore the dark zone in Fig.11 can be considered to be the crack of the inside of the specimen below the polished surface.

Figure 13 shows the OM micrographs for the part ahead of the crack tip for the 0.01wt% and 0.4wt% specimens at the onset of non-linearity, which were observed on the polished surface of the edge of the ENF specimens. The dark zone ahead of the crack tip was also observed in both cases as well as the 1.0wt% specimen. It can therefore be noted that the mode II crack began to occur at the onset of non-linearity regardless of the MPS concentration, as well as the mode I crack. However, very few micro cracsk were observed in the fiber strand ahead of the crack tip in the mode II case, even for the lower MPS concentration specimen.

Figure 14 shows the relation between the initiation values of mode II fracture toughness, G_{IIC}, and the MPS concentration, with the comparison of G_{IC}. The G_{IC} and G_{IIC} were calculated at the onset of non-linearity that were corresponding to the initiations of the crack occurrence in both cases. The G_{IIC} was clearly higher than G_{IC} regardless of the MPS concentration, and the G_{IIC} increased with an increase in the MPS concentration, although G_{IC} decreased.

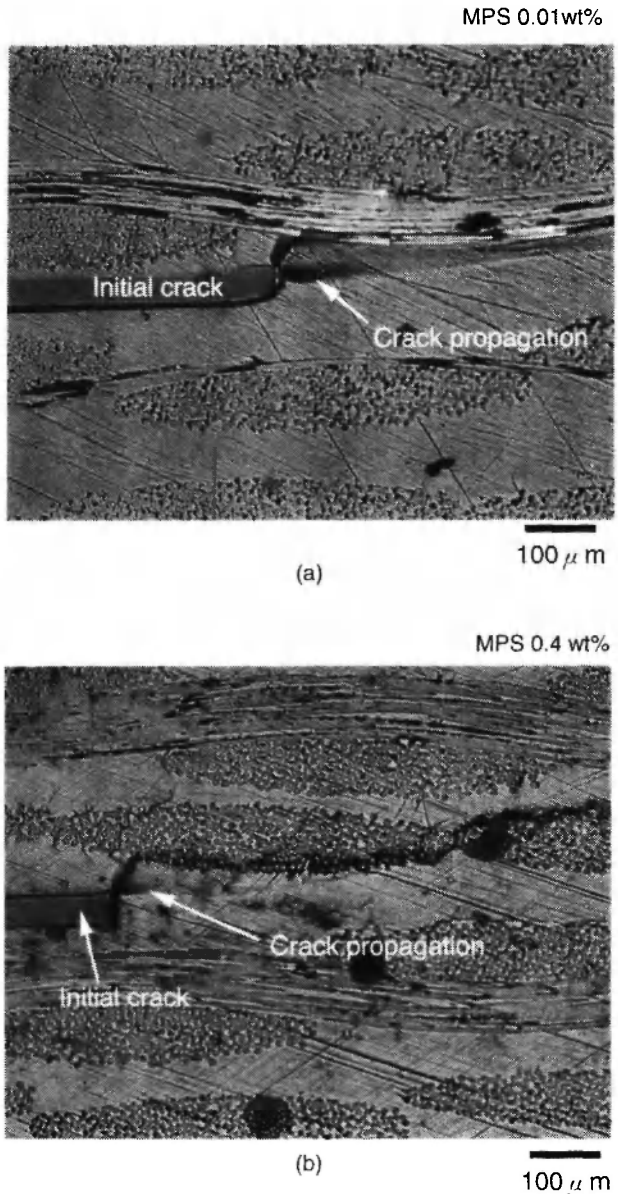

Fig. 13: OM micrographs of the part ahead of initial crack tip at the onset of the non-linearity in mode II crack initiation for (a) MPS 0.01wt% and (b) MPS 0.4wt% specimens of plain glass woven fabric composites .

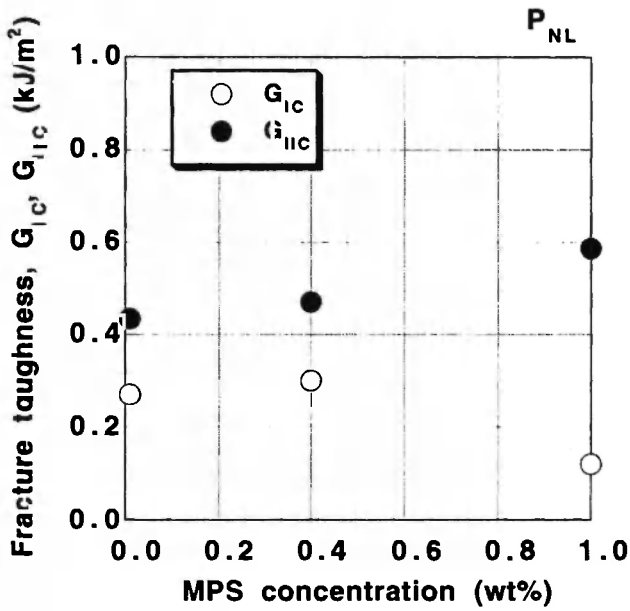

Fig. 14: Relation between initiation values of mode II fracture toughness and MPS concentration of plain glass woven fabric composites.

4. DISCUSSION

The low MPS concentration specimen displayed higher G_{IC} than the high MPS concentration specimen. This was attributed to the occurrence of the micro crack which was dependent on the MPS concentration, i.e. the adhesion between fiber and matrix. The fracture energy spent in the form of the large damage zone ahead of the crack tip by the occurrence of the micro crack in the fiber strands caused the higher fracture toughness in the low MPS concentration specimen in the mode I fracture.

As opposed to the mode I case, G_{IIC} increased with increase in the MPS concentration. The different fracture mechanism existed in the mode II crack initiation. The G_{IIC} was directly dependent on the interfacial adhesion between fiber and matrix, because the contribution of the fracture energy for forming the damage zone ahead of the crack tip was very small and the crack initiated to the fiber strand in all types of specimens.

The definite difference of the fracture mechanisms between mode I and mode II was the dependence of the form of the damage zone ahead of the crack tip on the MPS concentration. In the mode I fracture, the damage zone ahead of the crack tip was formed by the occurrence of the micro crack, and the size of the damage zone was dependent on the MPS concentration. On the other hand, in the mode II fracture, the micro crack in the fiber strand was not clearly observed and

the size of the damage zone was independent of the MPS concentration, so that the material strength itself affected G_{IIC}. Therefore, it can be concluded that the mode I and mode II fracture behaviors of the woven fabric composites are energy and strength-controlled types, respectively.

5. CONCLUSIONS

Mode I and mode II interlaminar fracture behavior of plain glass woven fabric composites with different silane concentrations was investigated in this paper. The fractographic observations using the optical microscope were conducted on the part ahead of the crack tip, in order to identify the mechanisms of the mode I and mode II crack initiations.

Both the mode I and mode II cracks initiated at the onset of non-linearity in the load-displacement curve in each fracture toughness test of the glass woven fabric composites. The mode I interlaminar fracture toughness for the crack initiation decreased with an increase in the silane concentration treated on the glass fiber fabrics, however, the mode II interlaminar fracture toughness for the crack initiation increased when the silane concentration was increased. The mode II fracture toughness values were higher than the mode I fracture toughness for the crack initiation without respect to the silane concentration.

The mode I fracture toughness was correlated with the occurrence of the micro crack in the fiber strand, which was affected by the silane concentration (interfacial adhesion between fiber and resin). In the low silane concentration (poor interfacial adhesion between fiber and resin), many micro cracks occurred in the fiber strand. Then, the higher fracture toughness was obtained from the contributions of the fracture energy for forming a large damage zone ahead of the crack tip by the occurrence of the micro crack. On the other hand, in the mode II fracture, a few micro cracks occurred ahead of the crack tip, so that the significant damage zone for the fracture toughness was not formed ahead of the crack tip before the crack initiation without respect to the silane concentration. Then, the mode II fracture toughness was directly dependent on the interfacial adhesion between fiber and matrix.

REFERENCES

1. P.J. Hine, B. Brew, R.A. Duckett and I.M. Ward. Failure mechanisms in continuous carbon-fiber reinforced PEEK composites, *Composite Science and Technology*, **35**, 31-51 (1989).
2. P.J. Hine, B. Brew, R.A. Duckett and I.M. Ward. Failure mechanisms in carbon-fiber-reinforced poly(ether sulphone), *Composite Science and Technology*, **43**, 37-47 (1992).
3. R.A. Crick, D.C. Leach, P.J. Meakin and D.R. Moore. Interlaminar fracture morphology of carbon fiber/PEEK composites, *Journal of Materials Science*, **22**, 2094-2104 (1987).
4. H. Wittich and K. Friedrich. Interlaminar fracture energy of laminates made of thermoplastics impregnated fiber bundles, *Journal of Thermoplastic Composite Materials*, **1**, 221-231 (1988).
5. M. Hojo and T. Aoki. Thickness effect of double cantilever beam specimen on interlaminar fracture toughness of AS4/PEEK and T800/epoxy laminates, ASTM STP 1156, 1993, 281-298.
6. W.D. Bascom, J.L. Bitner, R.J. Moulton and A.R. Siebert. The interlaminar fracture of organic-matrix, woven reinforcement composites, *Composites*, **11**, 9-18 (1980).
7. J.K. Kim, C. Baillie, J. Poh and Y.W. Mai. Fracture toughness of CFRP with modified epoxy resin matrices, *Composite Science and Technology*, **43**, 283-297 (1992).
8. V.K. Srivastava and B. Harris. Effect of particles on interlaminar crack growth in cross-plies carbon-fiber / epoxy laminates, *Journal of Materials Science*, **29**, 548-553 (1994).
9. D.J.-P. Turmel and I.K. Partridge. Heterogeneous phase separation around fibers in epoxy/PEI blends and its effect on composite delamination resistance, *Composite Science and Technology*, **57**, 1001-1007 (1997).
10. A. Aksoy and L.A. Carlsson. Interlaminar shear fracture of interleaved graphite/epoxy composites, *Composite Science and Technology*, **43**, 55-69 (1992).
11. L.Y. Xu and C.H. Kou. Effect of the interfacial interleaf to the interlaminar fracture of a new BMI

matrix composites system, *Journal of Reinforced Plastics and Composites*, **13**, 509-540 (1994).
12. A.P. Mouritz, J. Gallapher and A.A. Goodwin. Flexural strength and interlaminar shear strength of stitched GRP laminates following repeated impacts, *Composite Science and Technology*, **57**, 509-522 (1997).
13. L.K. Jain and Y.W. Mai. On the effect of stitching on mode I delamination toughness of laminated composites, *Composite Science and Technology*, **51**, 331-345 (1994).
14. W.L. Bradley and R.N. Cohen. Matrix deformation and fracture in graphite-reinforced epoxies, ASTM STP 876, 1985, 389-410.
15. X.N. Huang and D. Hull. Effects of fiber bridging on G_{IC} of a unidirectional glass/epoxy composite, *Composite Science and Technology*, **35**, 283-299 (1989).
16. T.W.H. Wang and F.D. Blum. Interfacial mobility and its effect on interlaminar fracture toughness in glass-fiber-reinforced epoxy laminates, *Journal of Materials Science*, **31**, 5231-5238 (1996).
17. J.G. Funk and J.W. Deaton. The Interlaminar Fracture Toughness of Woven Graphite/Epoxy Composites, NASA Technical Paper 2950, 1989, 1-26.
18. S.L. Bazhenov. Strong bending in the DCB interlaminar test of thin E-glass woven-fabric-reinforced laminates, *Composites*, **22** (4), 175-280 (1991).
19. B.J. Briscoe, R.S. Court and D.R. Williams. The effects of fabric weave and surface texture on the interlaminar fracture toughness of aramid/epoxy laminates, *Composite Science and Technology*, **47**, 261-270 (1993).
20. R. Frassine and A. Pavan The combined effects of curing and environmental exposure on fracture properties of woven carbon/epoxy laminates, *Composite Science and Technology*, **51**, 495-503 (1994).
21. V. Chellappa and B.Z. Jang. Crack growth and fracture behavior of fabric reinforced polymer composites, *Polymer Composites*, **17** (3), 443-450 (1996).
22. N. Alif, L.A. Carlsson and L. Boogh. The effect of weave pattern and crack propagation direction on mode I delamination resistance of woven glass and carbon composites, *Composites*, **29B**, 603-611 (1998).
23. B.J. Briscoe and D.R. Williams. Acid-base interactions in the interpretation of aramid composite and fabric mechanics, *Journal of Adhesion Science Technology*, **5**, 23-38 (1990).
24. N. Alif, L.A. Carlsson and J.W. Gillespie, Jr. Mode I, mode II and mixed mode interlaminar fracture of woven fabric carbon / epoxy, ASTM STP 1242, 1997, 82.
25. T. Ohsawa, A. Nakayama, M. Miwa and A. Hasegawa. *Journal of Applied Polymer Science*, **22**, 3203-3212 (1978).
26. L.T. Drzal, M.J. Rich, J.D. Camping and W.J. Park. *35th SPI*, **20-C**, 1980, 1-7.
27. L.T. Drzal. *15th National SAMPE Technical Conference*, 1983, 190-201.
28. D.L. Caldwell and D.A. Jarvie. *33rd International SAMPE Symposium*, 1988, 1268-1275.
29. P.S. Chua and M.R. Piggott. *Composites Science and Technology*, **22**, 33-42 (1987).
30. B. Miller, P. Muri and L. Rebenfeld. *Composites Science and Technology*, **28**, 17-32 (1987).
31. U. Gaur and B. Miller. *Composites Science and Technology*, **34**, 35-51 (1989).
32. B. Miller, U. Gaur and D.E. Hirt. *Composites Science and Technology*, **42**, 207-219 (1991).
33. J.F. Mandell, J.H. Chen and F.J. McGarry. *International Journal of Adhesion and Adhesive*, **1**, 40-44 (1980).
34. Testing methods for mode I interlaminar fracture toughness of unidirectional fiber-reinforced polymer matrix composites, Japanese Industrial Standards (JIS. K7086, 1993, 1-62.